

# Domain Adaptation of Population-Based of Bolted Joint Structures for Loss Detection of Tightening Torque

**Samuel da Silva\***

Associate Professor  
Universidade Estadual Paulista  
Departamento de Engenharia  
Mecânica, Ilha Solteira, SP, Brasil  
Email: samuel.silva13@unesp.br

**Marcus Omori Yano**

Graduate Research Assistant,  
Universidade Estadual Paulista  
Departamento de Engenharia  
Mecânica, Ilha Solteira, SP, Brasil  
Email: marcus.omori@unesp.br

**Rafael de Oliveira Teloli**

Assistant Professor,  
FEMTO-ST Institute,  
CNRS/UFC/ENSMM/UTBM,  
Department of Applied Mechanics,  
Besançon, France.  
Email: rafael.teloli@femto-st.fr

**Gaël Chevallier**

Full Professor,  
FEMTO-ST Institute,  
CNRS/UFC/ENSMM/UTBM,  
Department of Applied Mechanics,  
Besançon, France.  
Email: gael.chevallier@femto-st.fr

**Thiago G. Ritto**

Associate Professor,  
Universidade Federal do Rio de Janeiro,  
Departamento de Engenharia Mecânica,  
Rio de Janeiro, RJ, Brasil  
Email: tritto@mecanica.ufrj.br

*This paper investigates how to improve the performance of a classifier of tightening torque in bolted joints by applying transfer learning. The procedure uses vibration measurements to extract features and to train a classifier using a Gaussian Mixture Model (GMM). The key to enhancing the surrogate model for torque loss detection is considering the bolted joint structures with more qualitative and quantitative knowledge as the source domain, where labels are known and the classifier is trained. After applying a domain adaptation method, it is possible to reuse this trained classifier for a target domain, i.e., a set of different limited data of bolted joint structures with unknown labels. Four different bolted joint structures are analyzed. The new experimental tests adopt a wide range of torque in the bolts to extract the features with the respective labels under safe or unsafe tightening torque. All combinations of possible source or target domains are considered in the application to demonstrate whether the method can aid the detection of the loss of tightening torque, reducing the learning steps and the training sample. A guidance list is discussed based on*

*this population-based SHM of bolted joint structures.*

## 1 Introduction

Bolted joint structures are widely used to provide structural strength and adequate stiffness [1], in addition to vibration damping [2]. It is therefore important to ensure the correct tightening torque in each joint. Unfortunately, a direct measure in each bolt may not be possible, either because of the large number of sensors required because of access difficulties, e.g., offshore in deepwater. Thus, several continuous monitoring methods for classifying each bolt's torque have been proposed in the last few years [3–5]. Among these methods, the ones based on low-frequency vibration are affordable and benefit from the same instrumentation used for regularly monitoring the structural health condition [6].

The methodology often applied considers a controlled shaker to excite a broad spectral frequency assuming a wide range of tightening torques, also controlled by a torque wrench. Feature extraction is performed using the vibration data sets, and the features are applied to train classifiers. Once these structural health classifiers are estimated,

---

\*corresponding author

they can be applied to assess the structural condition of the same bolted joint structure. As features, the modal parameters, time, or frequency aspects are widely used to perform this training or to correlate with tightening torque variations. Miguel et al. [7] demonstrated these ideas in a bolted joint structure named Orion beam [8]. This structure is formed by two aluminum beams joined by three bolts. The transmissibility function between the acceleration of the input excitation and the velocity at the beam's free end is used to extract a combination of natural frequencies as features. A Gaussian Mixture Model (GMM) was able to separate the states between two classes: safe torque (healthy) and unsafe torque (damaged). After learning a Kriging model, this surrogate model quantified the level of the tightening torque by stochastic interpolation. The results were acceptable with an adequate confidence level, considering the low level of tightening torque in cNm.

Unfortunately, these classifiers tend to fail when used in other similar bolted structures, and it is not feasible to generalize them. An alternative lies in retraining the classifiers with new data sets from these other structures, which can be expensive and require a lot of time. Transfer learning is an attractive methodology that has proven to be effective when applied in these scenarios to allow the reuse of the same previously trained classifier [9]. The idea is, from a source structure, i.e., a system containing a broad data set with known labels, to transfer the knowledge to a target structure with unlabeled conditions or insufficient data to assess its structural integrity. This methodology can provide a learning stage that reduces the dimension of the feature space and classifies similar structures adequately. Transfer learning via domain adaptation transforms source and target data sets to a latent space, minimizing the distance between both data sets [10].

Recently, population-based transfer learning was proposed through domain adaptation methods to mitigate the divergences between the probability distributions of data sets collected from different structures, allowing the classifier's generalization in the structural integrity evaluation. Different applications have been reported using transfer learning and domain adaptation in the SHM context, from mitigating temperature effects in impedance signatures [11] to improving the training for damage detection in bridges using hybrid data with a combination of numerical and experimental data [12], also including statistic alignment to make robust classifiers on unbalanced data in SHM of bridges [13], incomplete data of a population of aircraft tailplanes [14], and others.

Yano et al. [15] applied a domain adaptation method in a numerical model (source) and experimental data from a building structure with three floors (target). The numerical model was utilized as the source domain since several numerical simulations provided a significant data set to train and recognize different structural conditions. Modal parameters are used as features to compute a damage index and then evaluate the structural condition. The results have shown that the domain adaptation method improves the classifier's performance and regression for damage detection and quantifi-

cation steps compared to the analysis performed in the original space. This is the scenario in most real-world cases, where it is expensive or impossible to fully understand the situation using experimental data without a long-term historical measuring campaign.

Ritto et al. [16] showed an offshore application for drilling purposes that reuses data to aid in validating dynamic predictions for different drill string configurations and scenarios of length and diameter. The performance of three domain-adaptation methods was compared: transfer component analysis (TCA), maximum independence domain adaptation (MIDA), and geodesic flow kernel (GFK). A torsional model was used as the source domain, with the friction localization labels known to train a classifier to localize the torsional friction. During the drilling, geometrical parameters are altered, and the same classifier is transferred to other target domains, i.e., unlabelled conditions. The classifier's performance is enhanced when the domain adaptation is implemented to reuse previous knowledge in the source domain.

Digital twins (DT) aim to represent specific physical systems, such as bolted joint structures, by considering physical, virtual, and connection parts [17, 18]. The key ingredients of DTs include physical systems and sensing, computational models that handle uncertainties, and model updates as the physical twin changes over time [19]. Some authors are exploring the use of DTs in structural health monitoring (SHM) [20–23]. However, constructing a DT can be challenging, especially when it requires long-term data and significant time processing for complex dynamic systems. In this context, transfer-learning approaches can be helpful in extending the validity of DTs [16, 24], allowing previous knowledge to be reused to obtain new machine-learning models. The case of bolted joints described in this paper is an example that falls within this context. Thus, this paper investigates the benefits of the transfer component analysis (TCA) domain adaptation method [10] for detecting damage in four different bolted joint beams. Specifically, three of the beams have the same geometry, while the fourth has a different contact configuration. The experimental data used in this study have not been published before and emulate the gradual loss of tightening torque at the lap joint. The study trains a prior damage classifier based on one of the structures (source) and then uses domain adaptation to reuse the classifier for the remaining structures (targets). The results show that this approach improves damage detection, especially when the targets are assumed to be unlabeled and have incomplete data.

The paper is organized as follows: First, a background on transfer learning is presented to the reader. The following section summarizes a discussion on the population of bolted joints used with the modal procedure computed to extract the features used in the classification of the structural state of the joint. Then, the experimental setup and the proposed damage detection methodology are described. The results of the tightening loss torque detection methodology are illustrated for this set of structures. Finally, the final remarks and recommendations are discussed.

## 2 Background in Domain Adaptation and Transfer Component Analysis

From the SHM perspective, features extracted from different structures present divergences between their distributions that prevent the classifier generalization from correctly assessing the structural integrity. This exists mainly due to differences in their framework and operational and environmental conditions that can affect their structural behavior [25]. Hence, domain adaptation is a compelling solution to overcome the limitations of machine learning to investigate different structures with the same model/classifier.

Machine learning and transfer learning algorithms differ in some aspects. Simply put, using classical machine learning when one has a different setup is necessary to retrain the algorithm to obtain a new model/classifier. The idea is to calculate some features from a structure (source domain) in the original space when the healthy state and damaged condition, i.e., the safe and unsafe tightening torque, are completely labeled. A classifier trained in this condition usually yields good results. Unfortunately, the accuracy of the same classifier decreases if it is applied to another structure (target domain) with incomplete and unlabeled states. This is the case when a structure with another type of bolted connection is considered. Meanwhile, transfer learning proposes to transfer the relevant knowledge from the source domain to improve the performance of the target classifier, not requiring estimating a new one from scratch.

In 2010, Pan et al. [10] proposed a domain adaptation method called transfer component analysis (TCA) to reduce the divergences between the features determined based on the data sets collected. The main idea is to determine a nonlinear function  $\phi(\cdot)$  that maps the features from source ( $\mathbf{X}_s$ ) and target ( $\mathbf{X}_t$ ) domains to a subspace, named reproducing kernel Hilbert space ( $\mathcal{H}$ ), where the divergences between their marginal distributions are reduced ( $P(\phi(\mathbf{X}_s)) \approx P(\phi(\mathbf{X}_t))$ ).

The distance between the marginal distributions of the source and target features is determined through the maximum average discrepancy ( $\mathcal{M}$ ), which defines the average squared distance between features from source and target structures after their mappings to the subspace. This distance metric can be written as:

$$\mathcal{M}(P(\phi(\mathbf{X}_s)), P(\phi(\mathbf{X}_t))) = \left\| \frac{1}{n_s} \sum_{i=1}^{n_s} \phi(x_{s_i}) - \frac{1}{n_t} \sum_{j=1}^{n_t} \phi(x_{t_j}) \right\|_{\mathcal{H}}^2 \quad (1)$$

In this case, a kernel matrix ( $\mathbf{K}$ ) is applied for the probability distance estimation due to the lack of label knowledge from the target domain and the complexity of determining the mapping function. So, the maximum mean discrepancy can be defined as  $\mathcal{M}(P(\phi(\mathbf{X}_s)), P(\phi(\mathbf{X}_t))) = tr(\mathbf{KL})$ , where the  $\mathbf{L}$  matrix can be described as:

$$\mathbf{L}_{ij} = \begin{cases} \frac{1}{n_s^2}, & x_i, x_j \in \mathbf{X}_s \\ \frac{1}{n_t^2}, & x_i, x_j \in \mathbf{X}_t \\ -\frac{1}{n_s n_t}, & \text{otherwise.} \end{cases} \quad (2)$$

The features embedding into the reproducing kernel

Hilbert space is carried out based on a low-rank empirical kernel matrix  $\tilde{\mathbf{K}} = \mathbf{K}\mathbf{W}\mathbf{W}^T\mathbf{K}$ , which uses a transformation matrix  $\mathbf{W}$  to infer the mapping into a  $m$ -dimensional space ( $m \ll n_s + n_t$ ). Then, the distance can be rewritten as:

$$\mathcal{M}(P(\phi(\mathbf{X}_s)), P(\phi(\mathbf{X}_t))) = tr(\mathbf{W}^T\mathbf{K}\mathbf{L}\mathbf{K}\mathbf{W}) \quad (3)$$

The reduction of the estimated distance in equation (3) results in the mitigation of divergences between the marginal distributions from the structures analyzed. Also, it is necessary to preserve the properties of the attributes after performing their inference to the latent space. Therefore, TCA leads to an optimization problem that can be written as

$$\begin{aligned} \min_{\mathbf{W}} \quad & tr(\mathbf{W}^T\mathbf{K}\mathbf{L}\mathbf{K}\mathbf{W}) + \mu tr(\mathbf{W}^T\mathbf{W}) \\ \text{subject to} \quad & \mathbf{W}^T\mathbf{K}\mathbf{H}\mathbf{K}\mathbf{W} = \mathbb{I} \end{aligned} \quad (4)$$

where the first term is the distance metric  $\mathcal{M}$ , and the regularization is represented in the second term with  $\mu > 0$  as the trade-off parameter. In addition, the data variance is represented by  $\mathbf{W}^T\mathbf{K}\mathbf{H}\mathbf{K}\mathbf{W}$ , where  $\mathbf{H} = \mathbb{I} - (\frac{1}{n_s+n_t})\mathbf{1}$  is the centering matrix,  $\mathbb{I}$  is the identity matrix,  $\mathbf{1}$  is a matrix of ones.

In this case, the Lagrange multipliers can be used to solve this minimization problem that leads to a straightforward eigenproblem determination. Then, the eigenvalue problem can be written as:

$$[(\mathbf{K}\mathbf{L}\mathbf{K} + \mu\mathbb{I})^{-1}\mathbf{K}\mathbf{H}\mathbf{K}]\mathbf{W} = \lambda\mathbf{W} \quad (5)$$

where the transformation matrix  $\mathbf{W}$  is determined by the  $m$  leading eigenvectors, which infers the features mapping based on  $\mathbf{Q} = \mathbf{K}\mathbf{W}$ .

It is worth noting that deep learning models are commonly used to solve complex problems where simpler classifiers may not be effective. In our study, we employed a Gaussian Mixture Model (GMM) as a classifier, which has already been validated in previous publications for different purposes and has demonstrated superior performance for outlier detection when compared to other classifiers. Our contribution lies in applying transfer learning to combine this previously validated classifier with four different beams, enabling us to effectively detect outliers in each beam's behavior. For more details, readers are invited to refer to our recent publication [7].

## 3 Vibration-based Tightening Torque Loss Detection

This section explains the experimental setup of the sets of bolted joint structures investigated and the binary classifier algorithm to detect the state of the connection.

### 3.1 Orion beam

Figure 1 introduces the experimental setup. The test bench consists of the Orion beam, which has been presented

as a benchmark in Teloli et al. [8]. The beams are made of duraluminium with  $200 \times 30 \times 2$  [mm] dimensions. The tests were conducted considering the structure in the clamped-free condition. For this, one of the beams had a length of 40 mm attached to a solid aluminum block which, in turn, is directly coupled to the shaker's excitation axis (see Fig. 1(a)). In the nominal version of the Orion beam, the lap-joint consists of three M4 bolts (a central bolt and two external) spaced along a length of 30 mm and connected by contact patches that retain the contact in a square area of  $12 \times 12$  mm<sup>2</sup> (see Fig. 1(c), flat-patch assembly) with an extra thickness of 1 mm. The patches are only present on the beam connected to the shaker. A detailed description of the structure and the experimental protocol are available in Teloli et al. [26].

For the analysis conducted in this paper, three specimens of the Orion beam were manufactured, as illustrated in Fig. 1(b). These structures were called beam #1, #2, and #3. Although these systems have the same nominal dimensions, their vibration behavior is not necessarily the same due to variations in the manufacturing process. This also motivates the analysis carried out by this work. Notwithstanding, a beam #4 was also proposed **using the same components of the other beams, but without using patches in the contact region. It has the same dimensions as mentioned above and uses three bolts. Still, its main difference from the nominal Orion beam lies in the geometry of the contact interface, where no patches are present. Contact is made directly between a flat-flat interface with an area of  $30 \times 80$  mm<sup>2</sup> (see Fig. 1(c), flat-flat assembly). This new joint configuration used the subcomponents of beam #3, whereby the position of the clamped beam is flipped concerning its centerline, thus forming the flat-flat interface.**

For all structures experimentally tested in this paper, a white-noise Gaussian input at a controlled amplitude level of 4 m/s<sup>2</sup> RMS was used as base excitation. The base motion was conducted by a permanent magnetic shaker TIRA (TV Model 51120). A Polytec vibrometer PSV-500 with a 3D scanning laser is used to measure the velocity at the free end of the beams. A DJB Konic Shear type A/20 piezoelectric accelerometer monitors the acceleration at the base. A Bruel & Kjaer 2626 accelerometer preamplifier is also employed for signal conditioning. The experimental setup also includes a National Instruments acquisition system composed of CompactDAQ Chassis (NI cDAQ - 9134), C-Series Sound and Vibration Input Module (NI-9263), and C-Series Voltage Output Module (NI-9234).

The experimental campaigns are performed on eight sets of 16 measurements for each structure after complete assembly and disassembly, repeated on different days to obtain a total of 128 realizations for each torque level. All four structures have the same assembly protocol. On the one hand, the central bolt is fully tightened with a torque value of 80 cNm during the experimental campaign. On the other hand, the tightening torque applied on the external bolts ranges from 10 to 80 cNm with an increment of 5 cNm at each experimental run. It is essential to point out that after tests, each bolt's tightening torque is checked by a Lindstrom MA500-1 torque wrench.

### 3.2 Proposed Methodology

Figure 2 illustrates the proposed methodology to detect changes in the tightening torque of bolted joints using indirect vibration signals. The modal parameters in frequencies sensitive to the proposed changes are identified and extracted from the spectral transmissibility signals - higher bending modes, approximately around 700 and 1900 Hz since they stress the lap-joint area more distinctly.

In the learning phase, a GMM is estimated using the modal parameters over a labeled range of tightening torque variations to cluster the reference/healthy conditions where the torque is considered safe. Meanwhile, the binary classifier evaluates the unlabeled validation data sets in the testing phase. In this case, a threshold  $\beta$  is defined using a Chi-square ( $\chi^2$ ) hypothesis test to compare a score calculated by Mahalanobis squared distance, named here by  $\mathcal{D}$ . This classifier has already been proven helpful to this test-bed in previous applications [7, 27]. The readers can find more details in these previous papers.

Figure 3 shows the domain adaptation of two generic datasets of different bolted joint structures—the procedure described in Fig. 2 can be applied in the same dataset. If a different bolted joint structure is used, possibly a relearning step is required with additional data, becoming prohibitive at most times. A transfer learning procedure, generically described in Fig. 3, can be applied in that situation. The purpose is to map the features from the original to a latent space, typically reducing the dimension. If this procedure is well done, the same threshold can be used to cluster the data in the target domain using the classifier learned in the source domain.

## 4 Results

A set of four beams with bolted connections are used to obtain the necessary data for the present investigation. Figure 4 illustrates the natural frequencies of the 4th, 5th, and 6th modes of the set of beams as a function of the tightening torque from the range of 80 cNm - 10 cNm for Beam #1. These features are used for all four structures to compute a damage index due to the high sensitivity to the modifications of the tightening torque, as previously performed in Miguel et al. [7]. Based on the results, it is possible to see superposition in the upper quartile of the indices computed in the change tightening torque and the lowest quartile (even the median value). Between 80 and 60 cNm, the structure is assumed to be in a healthy operating condition. The evolution of the natural frequencies as a function of the tightening torque indicates that a pronounced change in the system's dynamics occurs from 25 cNm on (the rate of reduction in the values of the features increases). Thus, the following is established: the structure has a low damage level between 60 and 30 cNm but it can continue to operate. For smaller values, the classifier should detect the change in structural condition, i.e., indicate the presence of damage. Another important observation is that the dispersion of the same modal parameters differs depending on the beam analyzed.

Assuming Beam #2 as the source, Figure 5 shows the

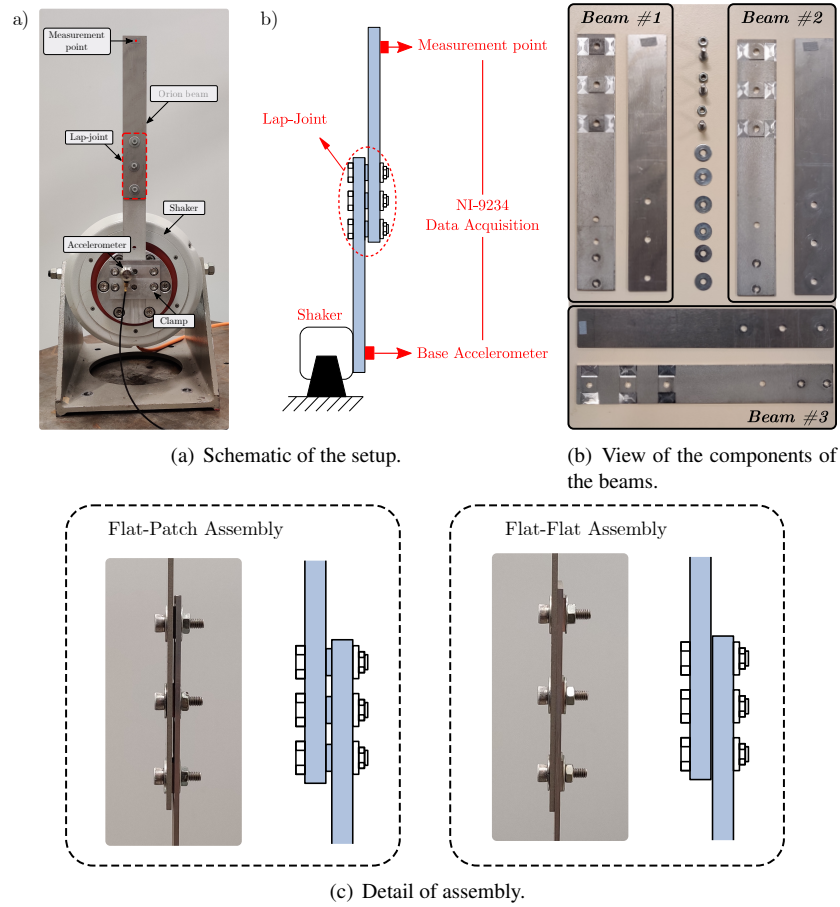


Fig. 1. Set of Orion beams used in the experimental tests.

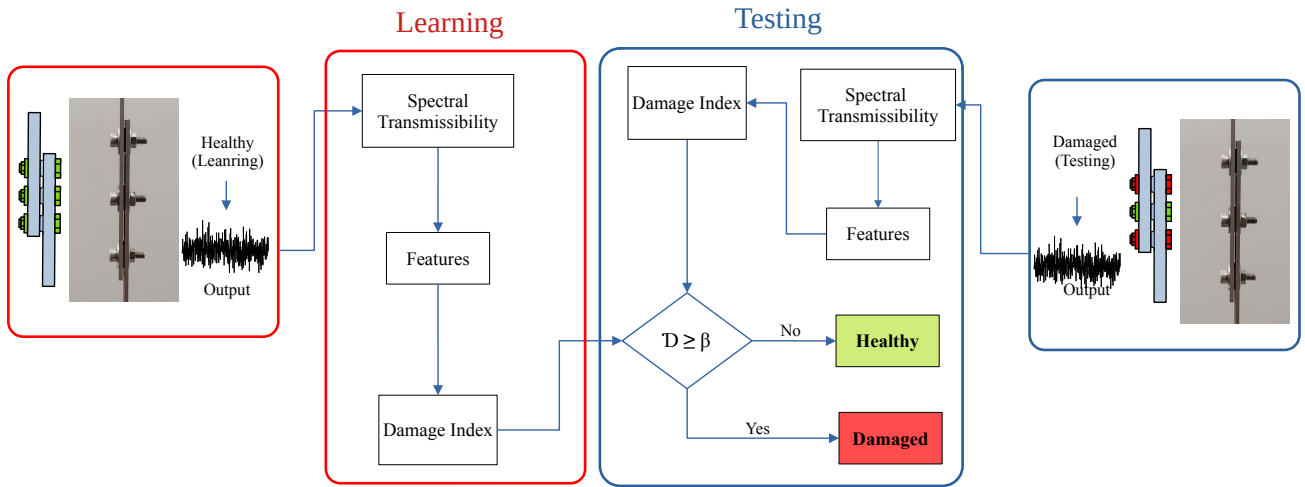


Fig. 2. Algorithm for detecting loss of the tightening torque based on vibration data in the source domain.

three natural frequencies considered as features, named  $\chi_1$ ,  $\chi_2$ , and  $\chi_3$  respectively, in the source domain. The central bolt holds the torque of 80 cNm, whereas the external ones were reduced to 25 cNm (damaged state). Once these data are labeled in each condition, a classification algorithm can

be trained to assess the structural condition of the bolted joint, i.e., if the tightening torque is under safe or unsafe conditions. Here, a GMM can provide acceptable results by training through 70% of healthy data, i.e., 448 samples labeled in the healthy state; the other 30%, i.e., 192 obser-

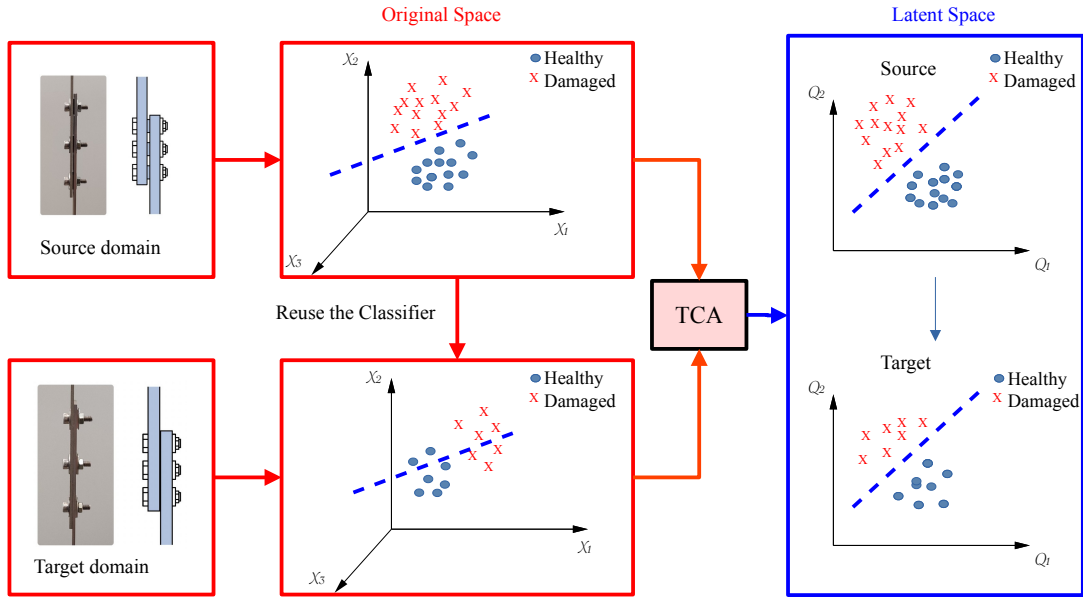


Fig. 3. Transfer component analysis (TCA) for detecting loss of the tightening torque based on vibration data from a source domain to a target domain.

vations, are used to verify the ability of the classification to give the correct assessment. Table 1 shows the training and validation schedule of the classifier algorithm. Figure 6 illustrates the score of the Mahalanobis squared distance. The threshold line is computed by a Chi-squared ( $\chi^2$ ) distribution with a probability of false alarm of 5%. A good outlier detection performance is achieved (as expected), with a false positive rate of 1.9% and a zero false negative rate.

The question now is: may this trained classifier detect the structural conditions of another structure with the same type of damage? Beam #1 is chosen as the target, assuming unlabeled conditions in each state of tightening torque. Figure 8 shows that the classifier trained on the source domain data fails to classify the structural conditions of the target domain. The damage condition is considered the same as the previous training, i.e., 25 cNm. Thus, a TCA domain adaptation is proposed for reusing the same GMM classifier trained in the source domain. Before the TCA application, a previous z-score normalization is performed in all data sets. Thus, by applying the TCA with a liner kernel, the latent space is obtained for both source and target domains. Figures 9 and 10 illustrate this transformation. The reduction from 3D-features to 2D-features in the new latent space after the TCA application is worth noting.

Figures 11 and 12 show that the same classifier trained on the source data can be used in the target data, presenting a satisfactory performance. In the latent space, the classifier's performance in the source beam tends to decrease due to an increase in the false negative rate. However, the source labels are known a priori and do not affect the correct assessment of its structural condition. Also, the source beam works well in the original space with the validation data. This is due to the compression of the space of features. A possible lack of some information and the high variability between the re-

sembles in different beams can affect the classification performance in the latent space. The point to note is whether we offer a classification on another beam without training for this condition, and the classifier scores indicate a possibility of detecting some situations. The following results show better performance of the classifier for smaller torque values with an adequate confidence level. Comparing the target data in a different beam, it is clear that the domain adaptation allows us to reuse the same classifier keeping a reasonable accuracy. The false positive rate in the target domain is 1.25%, which is associated with the significant data variability influencing the modal properties.

Note that the confidence levels on false positive and negative rates can also be influenced by choice of the structure adopted as the source and/or target. Figure 13 summarize the false positive and negative rates depending on different sources and target beams, assuming levels of tightening torque of 25, 20, and 15 cNm, respectively. Again, a classifier is trained using the knowledge from the source beam and applied to the target beams in the latent space. Based on the results, some conclusions can be listed. Beam #2 as source provided the best overall performance for detecting changes in the tightening torque. This source beam also allowed an adequate classification of the structural conditions of Beam #4, which is a structure with a different contact area, especially for lower torque values, such as 20 cNm and 15 cNm. Beam #2 presents more dispersion in the features space to capture the trends and classify the tightening torque state. On the other hand, beams #1 and #4, considered as a source, have a high false alarm rate on the other targets, indicating a lower performance of the classifier. Some aspects of the dispersion of the experimental data and contact interface conditions contribute to elaborate a more detailed discussion on this topic.

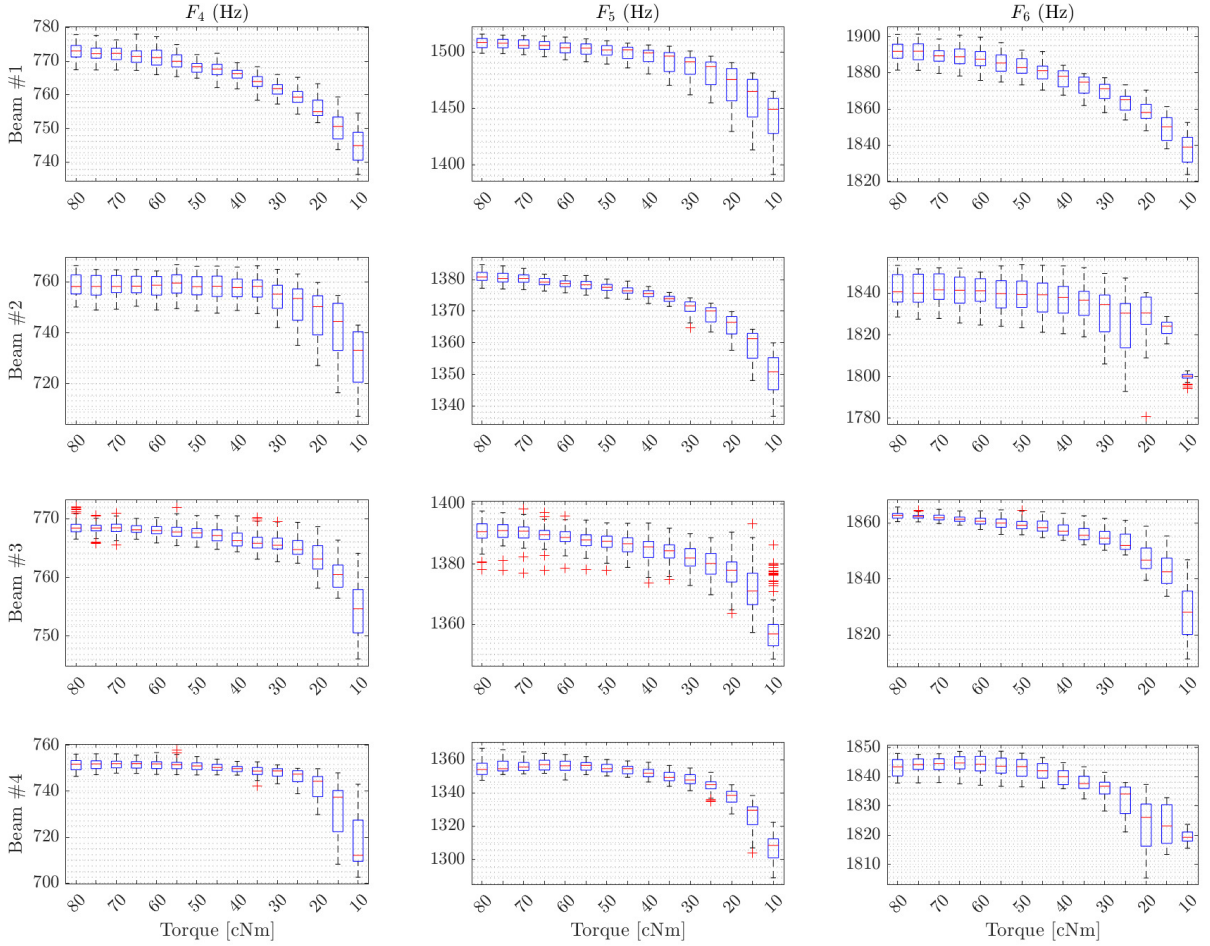


Fig. 4. Box plot of the natural frequencies for the source condition.

Table 1. Parameters for learning and validation.

Dataset	Condition	Samples	Range of torque (cNm)
Learning	Healthy	448	80, 75, 70, 65, 60
Validation	Healthy	192	80, 75, 70, 65, 60
Validation	Damaged	128	25

Figure 1(b) shows Beam #1 with black traces in the external patches. Thus, these are apparent traces of the wear caused by the friction between the surfaces. In previous work, this structure has undergone extensive experimental tests to characterize the nonlinear behavior of the Orion beam. Therefore, although design and geometry beam #1 is also an Orion beam, its dynamic behavior is different from the other beams and is influenced by this wear damage on its surface and the advanced time of its live cycle. These factors indicate a possible reason why the classifier performs more deficiently.

Beam #4 exhibits a greater amount of variability in its data compared to the other structures. This is because the

presence of patches in Orion beams leads to a contact interface that is concentrated only under the pressure cone formed by each bolt's contact area. As a result, Beam #4 has a non-uniform pressure distribution that affects its variability more significantly, especially when the tightening torque is lower. These physical differences among the structures impact the classifier's performance, resulting in discrepancies between beams used as source or target. Essentially, the classifier's ability to accurately distinguish between beams is affected by the dispersion in the data. Therefore, any differences in performance are more influenced by the classifier's ability than the TCA. Yano et al. [28] observed the similar effect analyzing two sets of unbalanced data in a bridge comparing

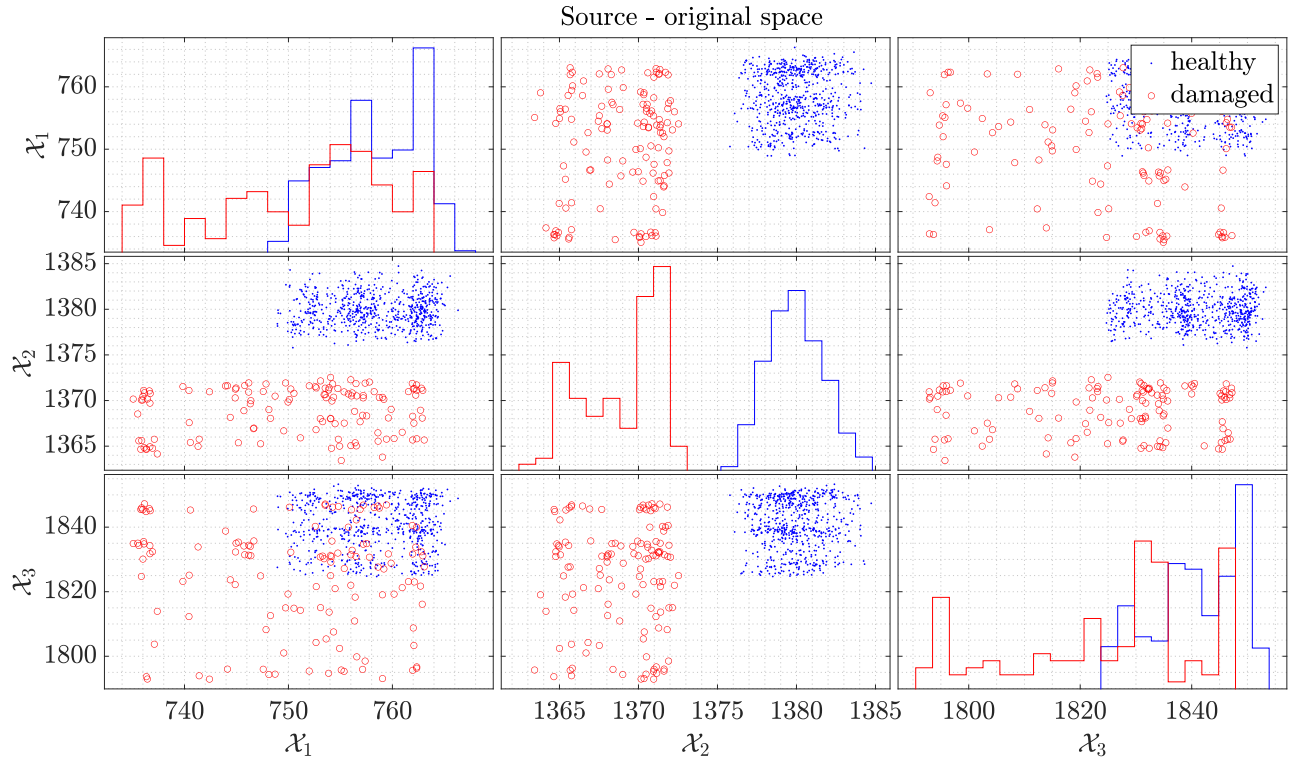


Fig. 5. Source assumed as Beam #2 for the structural condition healthy (torque in the range of 80 – 60 cNm) and damaged, when the torque is around 25 cNm - original space.

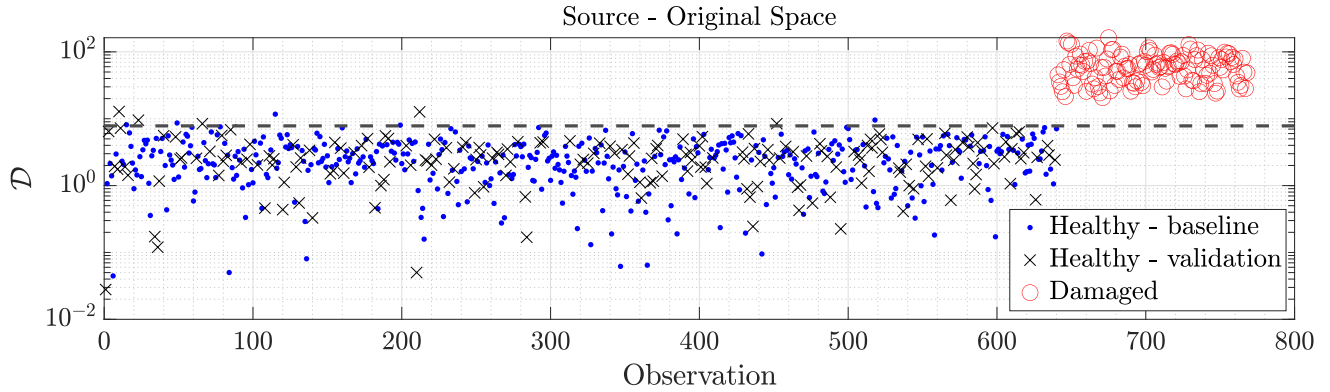


Fig. 6. Damage index computed with source domain (Beam #2) in original space, where  $--$  is the threshold. The false positive rate of 1.9%, and the false negative rate is zero.

unsupervised and supervised learning procedures, depending on the source and target bridge applied. A more suitable classifier for each situation's data core could enhance this performance.

## 5 Final Remarks

This paper has investigated a domain adaptation method called TCA for tightening detection in bolted joints. TCA was able to expand the usability of classifiers, trained in source data with known labels, to target data, with incomplete and unlabeled data, by mapping the features into a latent space. However, the results show that the choice of the

source database is important.

In this paper, we had access to 4 data sets that could be taken as source sets. A previous analysis shows that beam #1 had marks and that beam #4 had a completely different connection interface from the others; therefore, it was already expected that applying domain adaptation using these beams would present higher false alarm rates. On the other hand, beam #2 presents better conditions to be chosen as a source; in particular, beam #2 presents better implementation due to the high dispersion of the features using the same classifier. Here, the classifier was performed using the target, assuming only one tightening torque in each case once the TCA is a one-to-one procedure, i.e., source data is combined with

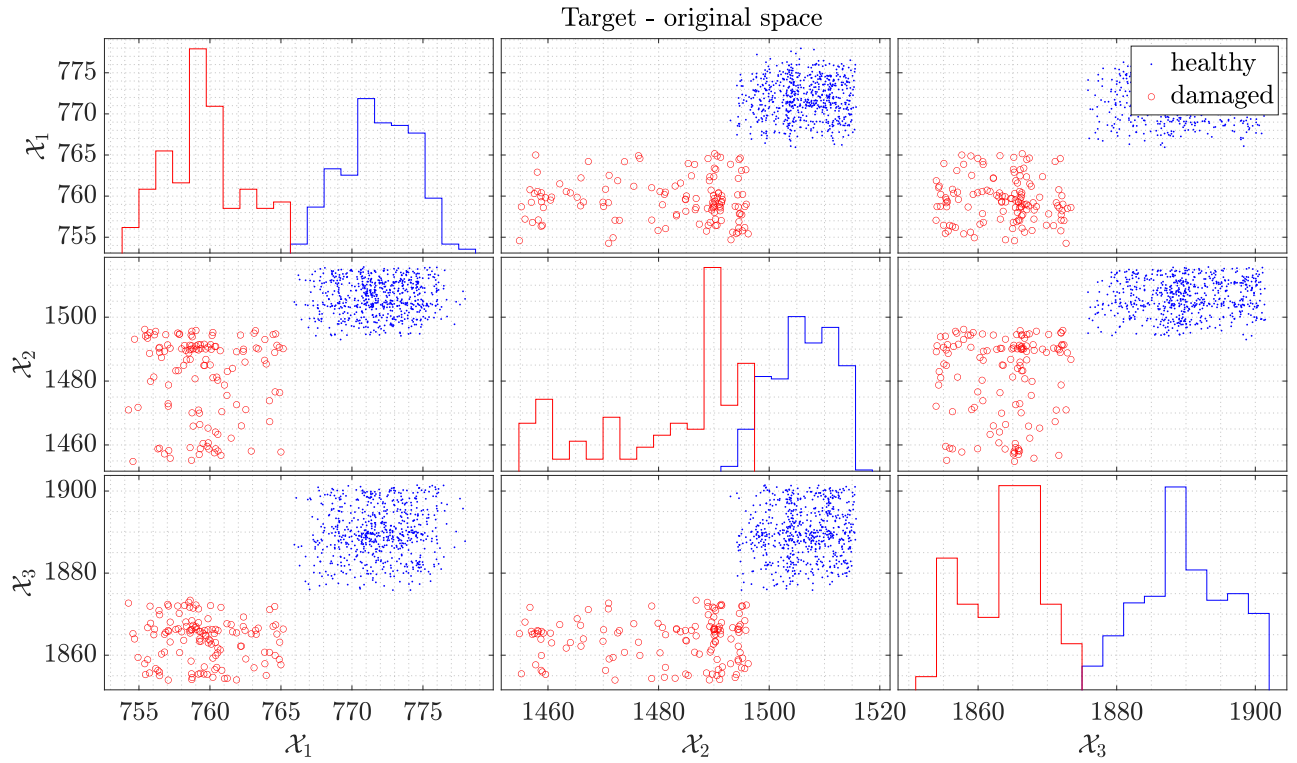


Fig. 7. Target assumed as Beam #1 for the structural condition healthy (torque in the range of 80 – 60 cNm) and damaged when the torque is around 25 cNm - original space.

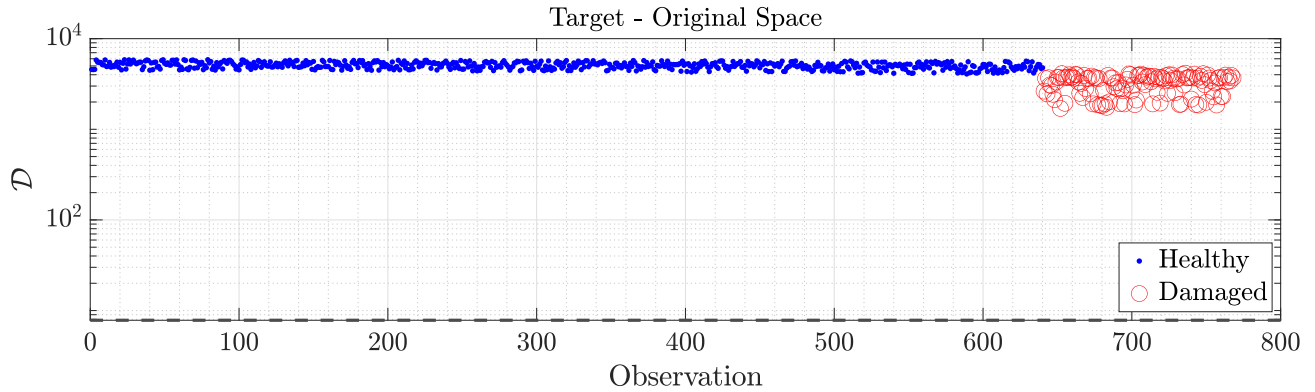


Fig. 8. Damage index computed with target domain (Beam #1) in original space, where — is the threshold. Classification failed using the previously trained Algorithm with a dataset of the source domain (Beam #2).

target data.

### Acknowledgements

The authors are thankful for the financial support provided by the Brazilian National Council for Scientific and Technological Development (CNPq) grant number 306526/2019-0 and São Paulo Research Foundation (FAPESP) grant number 19/19684-3 and 2023/00402-3. Marcus Omori Yano acknowledges the funding from the Coordenação de Aperfeiçoamento de Pessoal de Nível Superior (CAPES/Brazil)-Finance Code 001 and grant numbers 88882.433643/2019-01 and 88887.647575/2021-00. Samuel

da Silva and Gaël Chevallier thank the support from Consulat Général de France at São Paulo to the Chaire Franco-Bresiliennes des Universités de l’État de São Paulo.

### References

- [1] Kim, J., Yoon, J.-C., and Kang, B.-S., 2007. “Finite element analysis and modeling of structure with bolted joints”. *Applied mathematical modelling*, **31**(5), pp. 895–911.
- [2] Lacayo, R., Pesaresi, L., Groß, J., Fochler, D., Armand, J., Salles, L., Schwingshackl, C., Allen, M., and Brake, M., 2019. “Nonlinear modeling of struc-

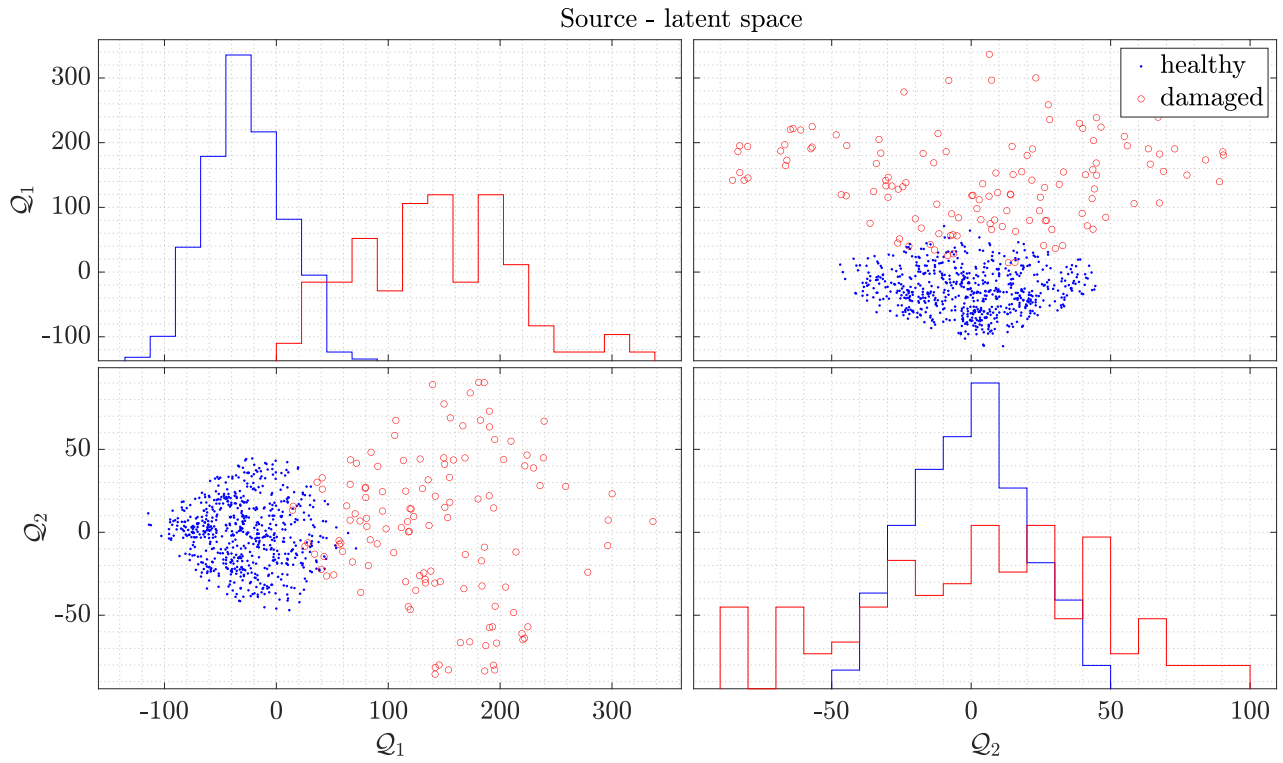


Fig. 9. Source assumed as Beam #2 for the structural condition healthy (torque in the range of 80 – 60 cNm) and damaged, when the torque is around 25 cNm - latent space.

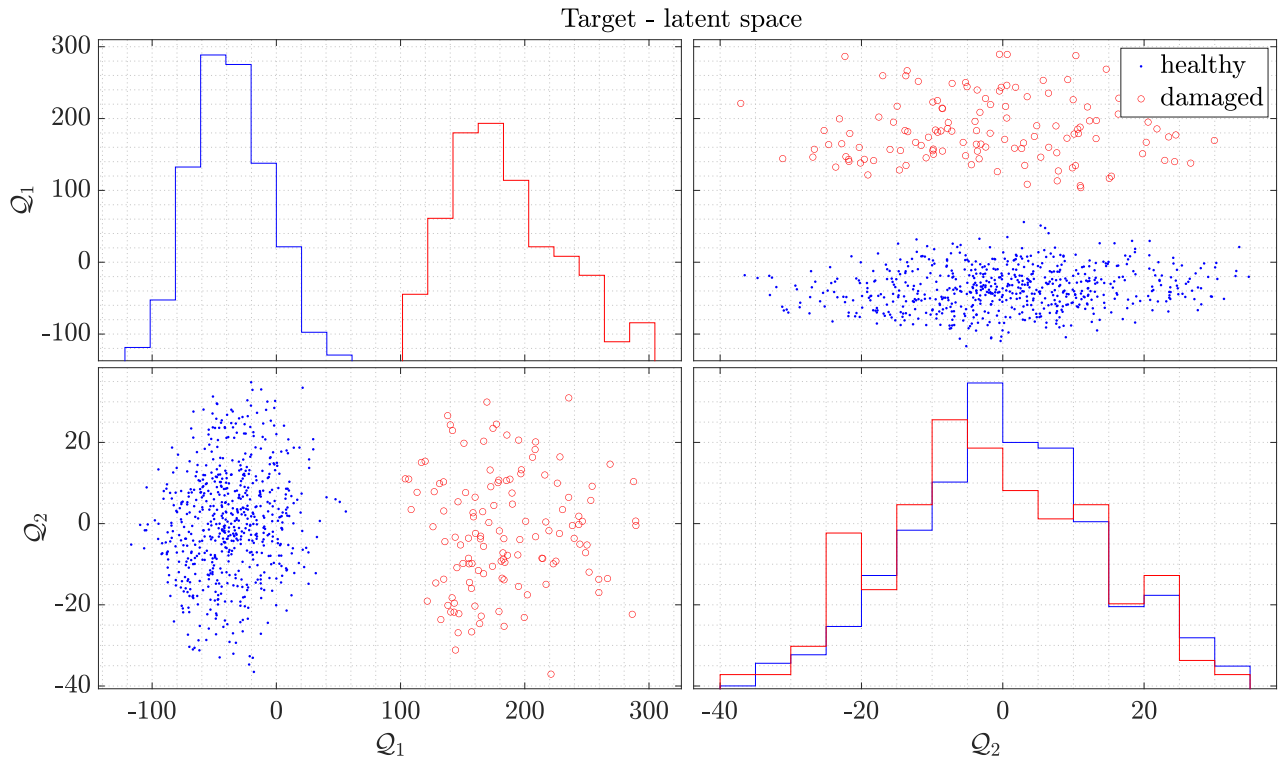


Fig. 10. Target assumed as Beam #1 for the structural condition healthy (torque in the range of 80 – 60 cNm) and damaged when the torque is around 25 cNm - latent space.

tures with bolted joints: A comparison of two ap-

proaches based on a time-domain and frequency-

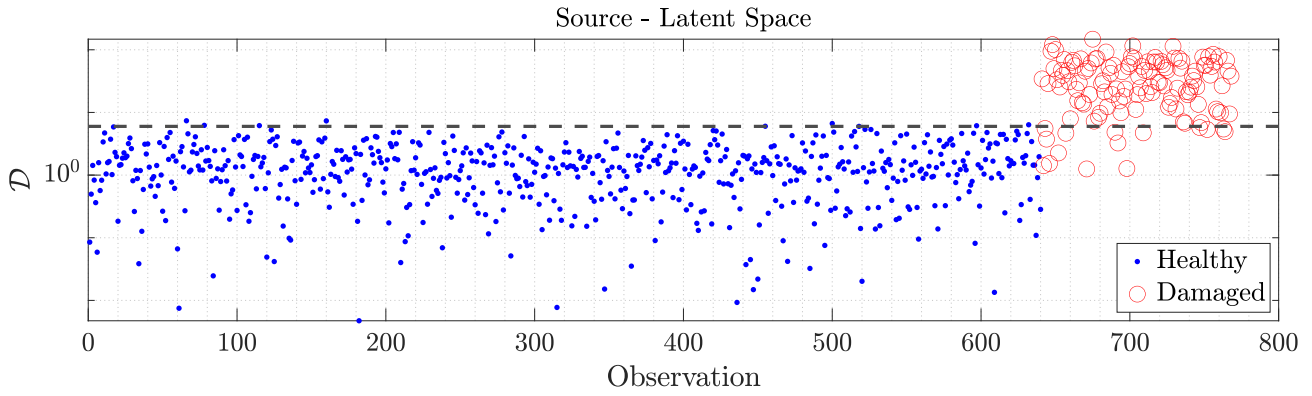


Fig. 11. Damage index computed with source domain (Beam #2) in latent space, where  $---$  is the threshold. The rate of false positive of 1.2%, and the rate of false negative is 7.0%.

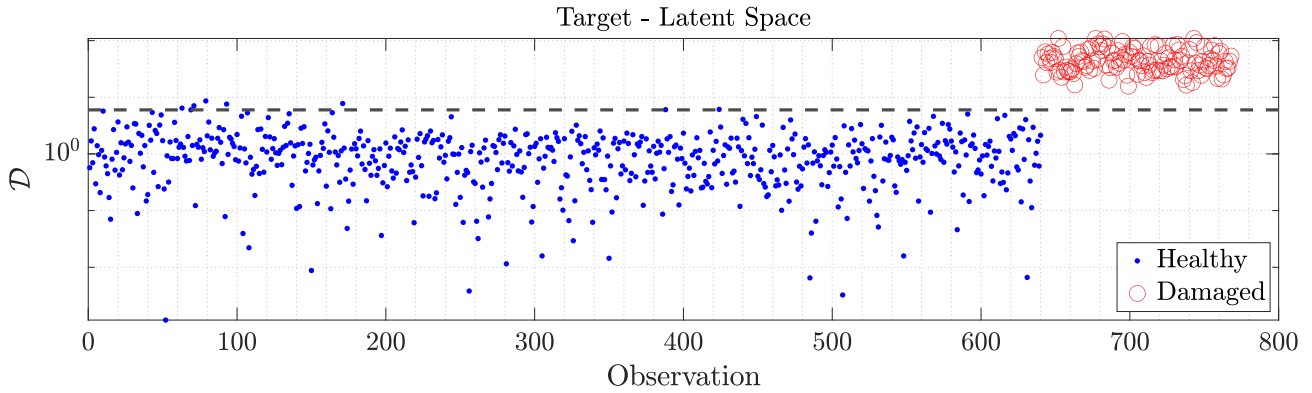


Fig. 12. Damage index computed with target domain (Beam #1) in latent space, where  $---$  is the threshold. The rate of false positive is 0.3%, and the rate of false negative is zero.

		Source beam						Source beam						Source beam			
		#1	#2	#3	#4			#1	#2	#3	#4			#1	#2	#3	#4
Target beam	#1		0.3%	1.1%	0.1%			0.0%	4.7%	1.7%				0.0%	8.7%	7.0%	
	#2	21.5%		14.8%	5.1%			0.0%		53.9%	44.5%			0.0%	64.4%	54.8%	
	#3	13.4%	2.5%		3.4%			12.9%	1.7%		5.8%			10.3%	0.6%		10.9%
	#4	22.5%	3.3%	9.2%				13.9%	0.4%	5.4%				3.1%	0.0%	1.7%	
			0.0%	0.0%	0.0%			0.0%	0.0%	0.0%	0.0%			0.0%	0.0%	0.0%	

(a)
(b)
(c)

Fig. 13. Performance of the classifier for different target domains assuming unsafe torque of (a) 25 cNm, (a) 20 cNm, (c) 15 cNm - latent space. ■ is the false positive rate, and ■ is the false negative rate.

domain solver”. *Mechanical Systems and Signal Processing*, **114**, pp. 413–438.

- [3] Huang, J., Liu, J., Gong, H., and Deng, X., 2022. “A comprehensive review of loosening detection methods for threaded fasteners”. *Mechanical Systems and Signal Processing*, **168**, p. 108652.

- [4] Kim, Y.-S., and Na, W. S., 2022. “Development of a portable damage detection system based on electromechanical impedance technique for monitoring of bolted joint structures”. *Journal of Intelligent Material Systems and Structures*, **33**(20), pp. 2507–2519.

- [5] Ziaja, D., and Nazarko, P., 2021. “Shm system for

- anomaly detection of bolted joints in engineering structures”. *Structures*, **33**, pp. 3877–3884.
- [6] Pal, J., Sikdar, S., and Banerjee, S., 2022. “A deep-learning approach for health monitoring of a steel frame structure with bolted connections”. *Structural Control and Health Monitoring*, **29**(2), p. e2873.
- [7] Miguel, L. P., Teloli, R. O., da Silva, S., and Chevallier, G., 2022. “Probabilistic machine learning for detection of tightening torque in bolted joints”. *Structural Health Monitoring*, **21**(5), pp. 2136–2151.
- [8] Teloli, R. O., Butaud, P., Chevallier, G., and da Silva, S., 2022. “Good practices for designing and experimental testing of dynamically excited jointed structures: The orion beam”. *Mechanical Systems and Signal Processing*, **163**, p. 108172.
- [9] Gardner, P., Liu, X., and Worden, K., 2020. “On the application of domain adaptation in structural health monitoring”. *Mechanical Systems and Signal Processing*, **138**, p. 106550.
- [10] Pan, S., Tsang, I., Kwok, J., and Yang, Q., 2011. “Domain adaptation via transfer component analysis”. *IEEE Transactions on Neural Networks*, **22**(2), pp. 199–210.
- [11] Silva, S. d., Yano, M. O., and Gonzalez-Bueno, C. G., 2021. “Transfer component analysis for compensation of temperature effects on the impedance-based structural health monitoring”. *Journal of Nondestructive Evaluation*, **40**(3), p. 64.
- [12] Figueiredo, E., Omori, M., da Silva, S., Moldovan, I., and Bud, M. A., 2022. “Transfer learning to enhance the damage detection performance in bridges when using numerical models”. *Journal of Bridge Engineering*.
- [13] Poole, J., Gardner, P., Dervilis, N., Bull, L., and Worden, K., 0. “On statistic alignment for domain adaptation in structural health monitoring”. *Structural Health Monitoring*, **0**(0), p. 14759217221110441.
- [14] Bull, L., Gardner, P., Dervilis, N., Papatheou, E., Haywood-Alexander, M., Mills, R., and Worden, K., 2021. “On the transfer of damage detectors between structures: An experimental case study”. *Journal of Sound and Vibration*, **501**, p. 116072.
- [15] Yano, M. O., da Silva, S., Figueiredo, E., and Villani, L. G. G., 2022. “Damage quantification using transfer component analysis combined with gaussian process regression”. *Structural Health Monitoring*, **0**(0), p. 14759217221094500.
- [16] Ritto, T., Worden, K., Wagg, D., Rochinha, F., and Gardner, P., 2022. “A transfer learning-based digital twin for detecting localised torsional friction in deviated wells”. *Mechanical Systems and Signal Processing*, **173**, p. 109000.
- [17] Grieves, M., 2014. “Digital twin: manufacturing excellence through virtual factory replication”. *White paper*.
- [18] Grieves, M., and Vickers, J., 2017. “Digital twin: mitigating unpredictable, undesirable emergent behavior in complex systems”. In *Transdisciplinary perspectives on complex systems*. Springer, pp. 85—113.
- [19] Ritto, T. G., and Rochinha, F. A., 2021. “Digital twin, physics-based model, and machine learning applied to damage detection in structures”. *Mechanical Systems and Signal Processing*, **155**, p. 107614.
- [20] Wagg, D., Worden, K., Barthorpe, R., and Gardner, P., 2020. “Digital twins: State-of-the-art and future directions for modelling and simulation in engineering dynamics applications”. *ASME*, **6**(3), p. 030901.
- [21] Hughes, A., Bull, L., Gardner, P., Dervilis, N., and Worden, K., 2022. “On robust risk-based active-learning algorithms for enhanced decision support”. *Mechanical Systems and Signal Processing*, **181**.
- [22] Rojas-Mercedes, N., Erazo, K., and Di Sarno, L., 2022. “Seismic fragility curves for a concrete bridge using structural health monitoring and digital twins”. *Earthquake and Structures*, **22**(5), pp. 503–515.
- [23] Longman, R., Xu, Y., Sun, Q., Turkan, Y., and Riggio, M., 2023. “Digital twin for monitoring in-service performance of post-tensioned self-centering cross-laminated timber shear walls”. *Journal of Computing in Civil Engineering*, **37**(2).
- [24] Teng, S., Chen, X., Chen, G., and Cheng, L., 2023. “Structural damage detection based on transfer learning strategy using digital twins of bridges”. *Mechanical Systems and Signal Processing*, **191**.
- [25] Gardner, P., Bull, L., Gosliga, J., Dervilis, N., and Worden, K., 2021. “Foundations of population-based shm, part iii: Heterogeneous populations – mapping and transfer”. *Mechanical Systems and Signal Processing*, **149**.
- [26] Teloli, R. O., Butaud, P., Chevallier, G., and da Silva, S., 2021. “Dataset of experimental measurements for the orion beam structure”. *Data in Brief*, **39**, p. 107627.
- [27] Ramasso, E., Denœux, T., and Chevallier, G., 2022. “Clustering acoustic emission data streams with sequentially appearing clusters using mixture models”. *Mechanical Systems and Signal Processing*, **181**, p. 109504.
- [28] Omori, M., Figueiredo, E., da Silva, S., and Cury, A., 2022. “Foundations of transfer learning for structural health monitoring of bridges”. *Mechanical Systems and Signal Processing*.